Surface Electronic Properties of Baltic Coastal Sands of Latvia

YURI DEKHTYAR[1], RENĀTE KALNIŅA[2], MARKS GOROHOVS[1], HERMANIS SOROKINS[1], MĀRIS DORTIŅŠ[1], ARTŪRS MAMAJEVS[1], SERGEI RASHKEEV[3], ELIZABETE SKREBELE[1], IGORS KOZAKS[1]

[1]Mechanical and Biomedical Engineering Institute,
Riga Technical University,
Riga, 6B Ķīpsalas Street, LV-1048,
LATVIA

[2]Latvian Maritime Academy,
Riga Technical University,
Riga, 6B Ķīpsalas Street, LV-1048,
LATVIA

[3]Materials Science and Engineering Department,
University of Maryland,
College Park, MD, 20742,
USA

Abstract: - Quartz sands are widely present in natural and engineered systems, yet their surface electronic properties remain poorly constrained in natural coastal environments. In this study, quartz-rich sands from four sectors of the Latvian Baltic Sea coast were investigated using photoelectron emission spectroscopy and Kelvin probe force microscopy to assess electron work function, surface potential, and near-edge electronic states. All samples exhibit a common quartz-dominated electronic structure; however, measurable differences arise from variations in defect-state density and surface potential organization. Sands from Salacgriva show a lower and more uniform work function and surface potential, whereas sands from Riga, Ventspils, and Liepaja display progressively greater electronic heterogeneity. These results demonstrate that coastal environmental conditions can induce systematic variations in the surface electronic properties of natural sands, with implications for electron–ion exchange processes and filtration-related applications.

Key-Words: - Quartz sand, Surface electronic properties, Electron work function, Surface potential, Electronion exchange, Coastal sediment.

Received: September 22, 2025. Revised: January 7, 2026. Accepted: June 4, 2026. Published: July 16, 2026.

1 Introduction

Quartz sands dominate many coastal systems and represent the product of prolonged weathering, transport, and abrasion, processes that continuously reshape grain surfaces and modify their chemical and physical reactivity, [1], [2], [3]. Although quartz is mineralogically simple, its surface can host a wide variety of structural defects, impurity centers, adsorbates, and hydration structures that collectively influence how the material interacts with ions and redox-active species in natural waters, [4], [5], [6]. The behaviour of insulating minerals such as quartz is strongly influenced by charge-trapping sites within both the surface and subsurface volume extending up to the charge-screening length, which can reach several micrometers, [7]. These traps arise from vacancies, interstitials, substitutional impurities, or complex defect clusters, and their energetic depth within the wide SiO_2 bandgap (≈8–9 eV) controls electron lifetimes and mobility, [8], [9]. Small variations in defect populations or surface termination can therefore produce measurable differences in surface potential and electron-transfer energetics, making quartz sand a sensitive indicator of environmental modification. These surface electronic characteristics are particularly important in processes such as heavy-ion adsorption, redox transformations, electrostatic binding, and catalytic interfacial reactions, where charge transfer and defect-mediated interactions largely determine efficiency, [10], [11]. Despite this relevance, the

electronic surface properties of natural quartz sands, such as surface potential, defect-state density, and work function, remain poorly characterized in natural coastal sediments.

The Baltic Sea provides an especially suitable setting to investigate these processes. Unlike fully marine systems, it is a brackish, semi-enclosed basin with strong riverine input, pronounced salinity gradients, heterogeneous wave energy, and abundant glacial sediments, [12]. Along the Latvian coastline, these environmental contrasts produce two fundamentally different coastal regimes: open-sea beaches exposed to energetic wave conditions, and Gulf of Riga beaches, where hydrodynamics are weaker, water is less saline, and river discharge plays a stronger role. Such differences in abrasion intensity, biological influence, hydration layers and surface coatings are expected to alter the density and arrangement of near-surface electronic states, even when the bulk mineralogy remains consistently quartz-rich, [13], [14]. However, whether these contrasting environments lead to measurable differences in electron-surface energetics has never been evaluated.

This study addresses this gap by providing the first comparative assessment of the surface electronic properties of quartz-rich sands from four environmentally distinct locations spanning both the open Baltic Sea and the Gulf of Riga sectors. The aim is to determine whether naturally occurring Baltic sands exhibit measurable, environmentally driven variability in key electronic parameters, and to evaluate how such differences may influence processes involving electron–ion exchange.

2 Materials and Methods

The presented study evaluates natural quartz sand from four locations along the Latvian Baltic Sea shoreline by characterizing their electronic properties that may influence electron-ion exchange at mineral surfaces – specifically the work function, nanoscale surface potential, and the presence of defect-related electronic states. These parameters were investigated using near threshold photoelectron emission spectroscopy (PEES), from which the electron work function and differentiated spectral features were extracted, and Kelvin probe atomic force microscopy (KPFM), which provides nanoscale surface potential mapping. The methodological details are described in the following subsections.

2.1 Sampling Sites and Sample Collection

To capture the variability of environmental conditions influencing sand grain surfaces, samples were collected from four coastal sectors of Baltic Sea shore: Riga (central Gulf of Riga; 57.04° N, 24.08° E), Salacgriva (northern Gulf of Riga; 57.75° N, 24.36° E), Ventspils (north-western open Baltic Sea; 57.39° N, 21.56° E), and Liepaja (south-western open Baltic Sea; 56.52° N, 20.99° E). These locations span distinct hydrodynamic and depositional settings along the Latvian coast.

Sampling was performed within the active swash zone, where wave and wind-driven processes most strongly affect sediment surfaces. A 1 m² area was delineated at each location, approximately 1 m from the waterline, and material was collected to a depth of around 30 cm. Two replicate samples were taken within each sector at a spacing of roughly 5 m to account for local variability. All samples were sealed immediately in plastic containers to prevent contamination and underwent identical handling, preparation, and storage protocols to ensure internal comparability between sites.

To ensure consistency across analyses, all samples underwent identical preparation steps aimed at removing fines and surface contaminants while preserving the intrinsic surface characteristics of the quartz grains. First, the material was dry sieved through a calibrated 0.8 mm stainless-steel mesh to eliminate larger clasts and loose fine particles. The retained fraction was then dried at 105 °C for 24 hours in a laboratory oven (SNOL 58/350, Lithuania) to minimize uncontrolled moisture-related variability across samples, cooled to ambient temperature and were placed in sealed glass containers under laboratory ambient conditions until analysis.

2.2 PEES Measurement and Data Processing

PEES was used to evaluate the electronic surface properties of the sand samples, including the electron work function and the presence of localized electronic states near the valence band edge. In total, five subsamples from each of the four locations were analyzed. The sand grains were placed in shallow cup-shaped sample holders to provide a stable measurement surface.

The measurements were performed using a custom-built PE spectrometer developed at Riga Technical University. The system operates at a vacuum of approximately 10^{-5} mmHg to minimize electron scattering. UV photons were supplied by a 30 W deuterium lamp (L7296, Hamamatsu Photonics, Japan), and specific wavelengths (4.2–

6.2 eV) were selected using an MDR-2 monochromator (Russia) with automated scanning. The emitted photoelectrons were then collected under an acceleration voltage of approximately 3000 V and detected using an SEM-6M secondary electron multiplier (VTC Baspik, Russia), connected to a Robotron 20046 radiometer (VEB Robotron-Meßelektronik, Germany) and a Hamamatsu Photonics M8784 counting board (Japan). The photocurrent at each wavelength was measured with a Keithley 6485 picoammeter (USA), and the photon flux was calculated using the known spectral sensitivity of the photodiode to correct the PE spectra for the wavelength-dependent emission intensity.

To determine changes in surface charge, the electron work function (EWF) of electrons emitted under UV light can be calculated. The EWF is the minimum amount of energy required for an electron to escape from a solid. The work function can be determined based on the obtained data from photoemission spectroscopy and calculated as follows (1):

$$\frac{Y}{dY/_{dh\nu}} = \frac{1}{m}h\nu - \frac{\varphi}{m}, \quad (1)$$

where Y is quantum yield, the ratio between the amount of emitted quants to the amount absorbed, φ – photoelectric work function, $h\nu$ – photon energy, m – constant, dependent on the material structure.

To enhance the visibility of subtle electronic features, the acquired spectra were processed before analysis. A 7-point moving average filter was applied to reduce noise while preserving spectral shape. Additionally, the first numerical derivative *dI/dE* was then calculated to reveal inflection points associated with the valence band edge and to highlight the presence of defect-related or localized states not easily distinguishable in the raw spectra.

2.3 Kelvin Probe AFM Measurements

Kelvin probe atomic force microscopy (KPFM) was employed to measure the nanoscale surface potential of collected sand samples. For this, an atomic force microscope (Solver–P-47 Pro, NT-MDT, Russia) with NSG10/Pt scanning probes (TipsNano Co, Estonia) were used. Measurements were performed under ambient conditions.

Because KPFM requires a conductive pathway between the sample and the instrument grounding system, the grains were mounted on a conductive copper substrate. A thin layer of silver conductive paste was applied to the surface of the copper film to ensure electrical continuity, and individual sand grains were deposited onto the paste with sufficient spacing to prevent mutual electrostatic influence during measurement. KPFM scans were performed on isolated grains using a scan area of approximately 10 × 10 μm². This size was selected to capture representative nanoscale variations on the surface while avoiding steep topographical features near grain edges, which can distort the surface potential signal. Due to the high sensitivity of AFM to height variations, only sufficiently flat surface regions were analyzed.

The measurement principle relies on detecting the contact potential difference (CPD) between the conductive tip and the sample surface. Mean CPD values and standard deviations were calculated for multiple grains from each location to quantify average surface charging and nanoscale heterogeneity.

3 Results

The measurements described in the previous section yielded a set of electronic parameters that characterize the surface behavior of the sand grains from the four coastal locations. In this section, these results are presented and examined to identify systematic differences between the sampling sites and to determine how the observed electronic features relate to the ability of the grains to participate in electron–ion exchange.

3.1 Electron Work Function (PEES)

The EWF was determined from the PEES spectra for all sand samples. Figure 1 presents the typical emission spectra obtained from the four sampling locations, illustrating the differences in the low-energy cutoff region of photon energy used for EWF extraction. A comparative overview of the mean EWF values is shown in the bar chart in Figure 2.

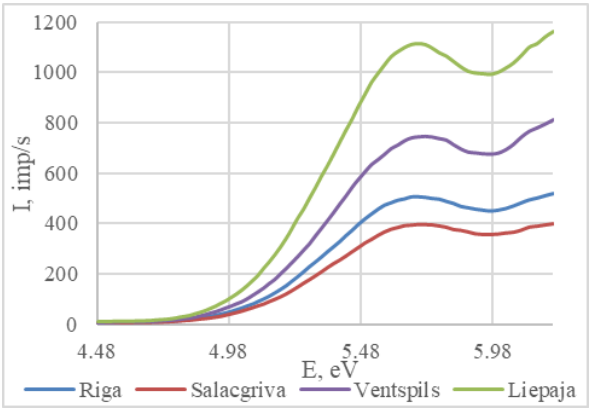

Fig. 1: Combined PEES spectra for Riga, Salacgriva, Ventspils, Liepaja

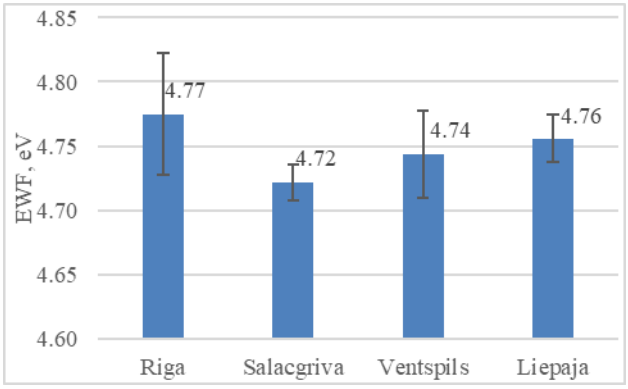

Fig. 2: Bar chart of EWF values

The electron work function (EWF) measurements reveal systematic, though in some cases subtle, differences between the coastal sectors. Among the four locations, Salacgriva exhibits the lowest mean EWF value (4.72 ± 0.01 eV), accompanied by the smallest standard deviation, indicating a highly uniform electronic surface state. The other three sites – Riga (4.78 ± 0.05 eV), Ventspils (4.74 ± 0.03 eV), and Liepaja (4.76 ± 0.02 eV) – display higher and mutually overlapping EWF values, suggesting broadly comparable surface energetics within the uncertainty of the measurements.

Because EWF error intervals overlap for most sites, statistical testing was applied to verify whether the observed differences are meaningful. Pairwise comparisons were performed at a nominal $\alpha = 0.05$; p-values are reported as descriptive, given multiple comparisons. Tests show that only two location pairs exhibit statistically significant differences ($p < 0.05$): Salacgriva-Riga ($p = 0.04$) and Salacgriva-Liepaja ($p = 0.02$).

All other pairings do not show a significant distinction between their EWF distributions. Although the Salacgriva-Ventspils means overlap due to the relatively high dispersion in the Ventspils dataset, Salacgriva remains statistically distinguishable from the other regions based on its combination of a lower and more tightly clustered EWF.

These findings suggest that Salacgriva sand has a distinct electronic surface structure relative to the other coastal sectors. A lower EWF indicates that electrons require less energy to escape from the surface, which may be associated with enhanced ability to participate in electron-transfer processes, which can lead to increased surface reactivity toward dissolved ions or greater likelihood of forming surface dipoles or polar adsorption sites, although it also depends on the density and accessibility of near-surface electronic states. In contrast, the sands from Riga, Ventspils and Liepaja share broadly similar EWF values, implying that their average surface electronic behavior is comparable despite environmental differences among the sites.

Overall, the combination of consistently low EWF, minimal variability, and confirmed statistical separability indicates that Salacgriva sand grains possess a more uniform and energetically accessible electron population. This distinguishes them from the three other studied regions and suggests that Salacgriva sediments may exhibit enhanced electron–ion exchange capability in natural aqueous environments.

3.2 Surface Potential (KPFM)

Kelvin probe AFM measurements were used to quantify the nanoscale surface potential of the sand grains through the contact potential difference (CPD). The CPD reflects local variations in the near-surface work function and the degree of surface charging or dipole orientation. Representative KPFM images for an individual grain are shown in Figure 3, illustrating both the topography and the corresponding CPD map obtained from the same region. These maps highlight the heterogeneous nature of the surface, with distinct nanoscale domains exhibiting different potential levels.

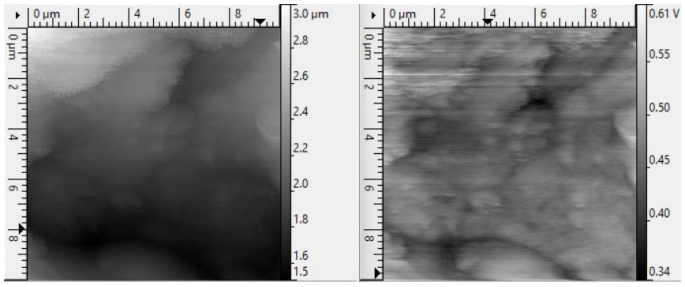
Fig. 3: Example AFM topography image (left) and corresponding CPD map (right)

CPD values, including mean surface potential and standard deviation for each of the four sampling locations, are summarized in a comparative bar chart presented in Figure 4.

The CPD measurements reveal clear differences between the coastal sectors, although not all variations are statistically significant. The Salacgriva samples exhibit the highest and most tightly clustered CPD values (0.720 ± 0.010 V), indicating a consistently elevated surface potential across individual grains. In contrast, the other three locations – Riga (0.434 ± 0.043 V), Ventspils (0.444 ± 0.067 V), and Liepaja (0.471 ± 0.070 V) – show substantially overlapping error intervals, all three exhibit broader potential distributions, indicating

greater nanoscale heterogeneity of their grain surfaces. Such variability may arise from differences in abrasion intensity, partial coatings, hydration films, or residual organics that introduce patchy charge distributions. Figure 5 shows potential distributions on Salacgriva samples. Figure 5 shows typical potential distributions on samples from all collection sites.

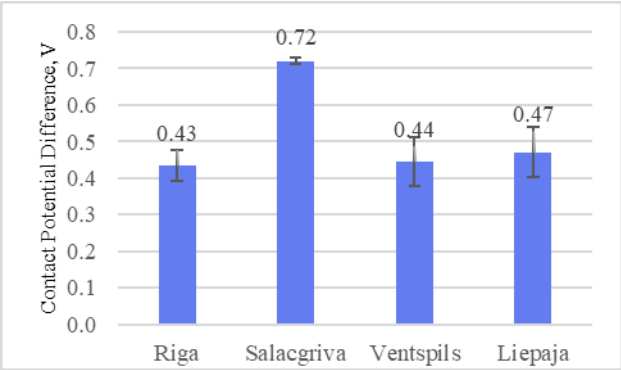

Fig. 4: Bar chart of CPD values by location

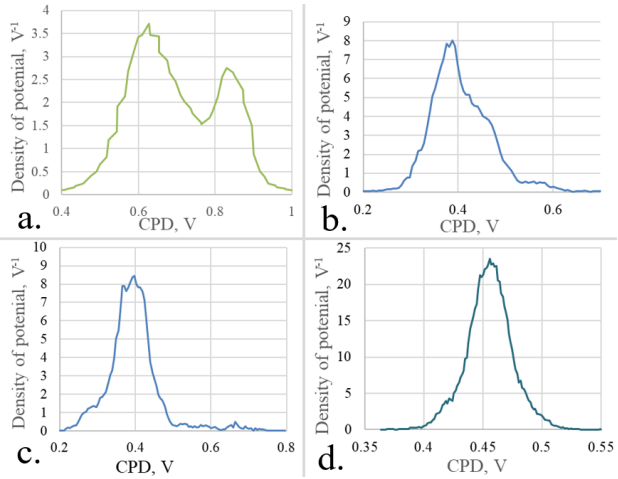

Figure 5: Typical potential distributions of sand samples: a. Salacgriva, b. Riga, c. Ventspils, d. Liepaja

Salacgriva stands out not only by its elevated mean CPD, but also by the shape of its potential distribution. Unlike the approximately Gaussian profiles observed for Riga, Ventspils and Liepaja, the Salacgriva grains consistently exhibit a bimodal potential distribution, with two distinct peaks centered near ~0.62 V and ~0.75-0.85 V.

The presence of two surface-potential states on multiple individual grains may suggest that Salacgriva sand possesses a more complex surface electronic structure. This may reflect the influence of fluvial input, biological films, or environmentally induced surface modifications that stabilize two preferential polarization states.

Together with the work-function data, the CPD measurements highlight that Salacgriva sands have the strongest and most consistent surface polarization, making it potentially more reactive in electrostatic or electron–ion exchange processes than the sands from the other coastal sectors.

3.3 Differentiated PEES Spectra Analysis

To resolve subtle variations in the electronic structure near the valence band edge, the PEES spectra acquired for all samples were smoothed using a 7-point moving average and numerically differentiated. The resulting first-derivative spectra for the four sampling locations are shown in Figure 6. Differentiation enhances weak inflection points associated with band-tail states, localized surface states and the main onset of photoemission, allowing the underlying electronic transitions to be examined with greater clarity than in the raw PEES curves.

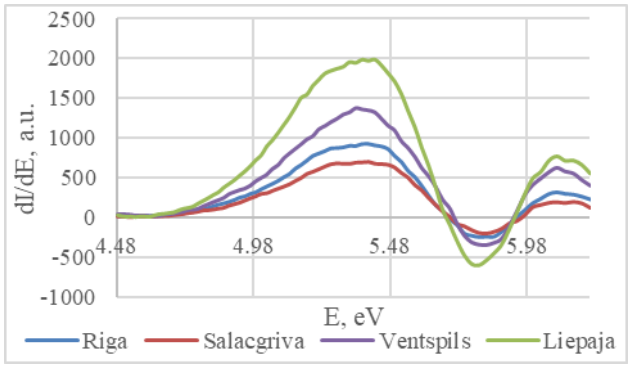

Fig. 6: Typical differentiated PEES spectra for all four locations

While the differentiated spectra already reveal qualitative differences, most notably the weaker and narrower features in Salacgriva and the stronger, broadened transitions in Liepaja, quantitative interpretation requires separating the overlapping electronic contributions. For this purpose, each differentiated spectrum was subjected to three-component deconvolution using a Gaussian peak model, using OriginPro software. Figure 7 shows the example of deconvoluted graph.

Initial unconstrained fits consistently converged toward three peaks centered at energies (E) of 4.90 eV, 5.28 eV, and 5.48 eV within a narrow energy range of ±0.1 eV across all samples. A three-component model was retained as the lowest-complexity fit that consistently captured the main derivative features across all samples. Gaussian deconvolution achieved R^2 values of 0.88-0.93 across all samples, with acceptably stable fits.

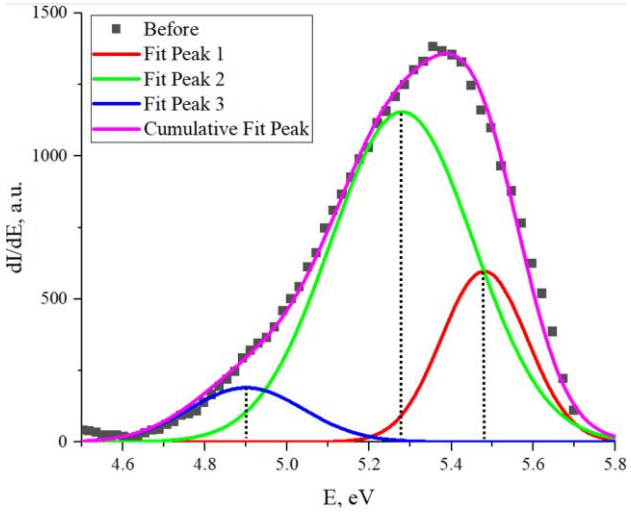

Fig. 7: Example of deconvoluted graph

These energies were consistent across all locations, indicating that the fundamental quartz-related electronic structure is preserved along the Latvian coast, and that variations may arise primarily from changes in the density and distribution of local electronic states, rather than from shifts in band-gap position. Specific energy positions are considered as near-edge electronic contributions relative to the valence-band onset rather than being assigned to specific defect types, as the exact energetic position of defect-related states in natural quartz may vary with local composition, structural disorder, and surface chemistry.

Table 1 presents the parameters for extracted fit peaks (Figure 7): area (A), height (h) and half-height width (h_1) of peak

Table 1. Parameters of deconvoluted peaks

Sample location site	E, eV	A	h	h_1
Riga	4.90	79.8	201	0.37
	5.28	292.5	788	0.35
	5.48	120.6	519	0.22
Salacgriva	4.90	32	88	0.35
	5.28	286	628	0.43
	5.48	71	316	0.21
Ventspils	4.90	66	180	0.33
	5.28	503	1159	0.41
	5.48	157	595	0.25
Liepaja	4.90	105	283	0.34
	5.28	785	1813	0.41
	5.48	199	937	0.2

Salacgriva consistently exhibits the lowest peak areas at 4.90 eV (A ≈ 32) and 5.48 eV (A ≈ 71), as well as the lowest overall derivative amplitude. This may be associated with a comparatively low density of localized electronic states contributing to photoemission near the valence-band onset and suggests a more ordered electronic surface structure.

In contrast, Liepaja shows the strongest deconvolution components, with the largest peak areas at 4.90 eV (A = 105), 5.28 eV (A = 785), and 5.48 eV (A = 199). Combined with broader derivative features, this reflects a high density of defect or near-edge electronic contributions and the most electronically heterogeneous surface behavior among the investigated locations.

Riga and Ventspils exhibit intermediate behavior. Riga shows moderate peak areas across all three energy positions, while Ventspils displays a particularly strong contribution at 5.28 eV (A = 503), together with elevated values at the other energies. Both locations therefore occupy a middle position in terms of near-edge electronic state density between Salacgriva (lowest) and Liepaja (highest).

4 Discussion

Results show that Baltic coastal sands along the Latvian coast share a common quartz-dominated electronic framework but differ significantly in the density, organization, and accessibility of near-surface electronic states, which are key determinants of electron–ion exchange. Quartz and other SiO_2 polymorphs exhibit a wide band gap (~8–9 eV) with relatively stable valence-band structure, so modest changes in local chemistry or microstructure are expected to primarily affect the population of electronic states close to the valence-band edge rather than the bulk band structure, [8]. In this context, the electron work function defines the energetic barrier for electron transfer across the surface, while the density and organization of surface electronic states determine how readily the material can participate in processes involving electron exchange, such as adsorption, charge transfer, and redox reactions, [15].

Deconvolution of the differentiated PEES spectra into three Gaussian components centered at 4.90, 5.28 and 5.48 eV for all four locations indicates that the energetic positions of the main valence-band onset and associated local states are invariant across Riga, Salacgriva, Ventspils and Liepaja. This invariance suggests that the underlying electronic structure is dominated by the intrinsic properties of quartz-rich silica, which exhibits a wide band gap and structural stability that are relatively insensitive to minor environmental variation. Although there is no single universal

database assigning exactly these three energies, prior studies indicate that optically and electronically active states associated with defects in SiO_2 occur within a similar ultraviolet energy range and contribute to near-edge photoemission behavior, [16], [17], [18]. Because the bulk quartz band structure remains stable, differences between sampling sites arise predominantly from variations in the areas and widths of these deconvoluted components, which may represent the density and degree of disorder of tail states and surface-localized states near the band edge. Such states are known to mediate adsorption, charge trapping, and electron–ion exchange processes at oxide and silicate, [19], [20].

Among the studied sites, Salacgriva shows the lowest EWF (4.72 eV) with the smallest variability, and t-tests confirm that it differs significantly from Riga and Liepaja. A lower EWF indicates a reduced energetic barrier for electron transfer, which may be compatible with more efficient charge exchange when the density of trap states is low. This interpretation is supported by the smallest deconvoluted peak areas, reflecting a relatively low presence of defects, thus more structurally ordered. KPFM provided additional evidence of surface order of Salacgriva sand, it displays a bimodal distribution highly associated with the CPD distribution, which typically reflects the presence of stable surface terminations or distinct dipolar configurations rather than random heterogeneity, which may be associated with hydroxylation and protonation states on silica surfaces, [21], [22]. Alternative explanations for the bimodal CPD, such as sand grain heterogenetic structures, cannot be excluded and is planned to be examined in follow-up works using complementary chemical/morphological characterization. Taken together, results indicate that Salacgriva sand may support efficient and predictable electron–ion exchange, with minimal deep trapping and a more ordered interfacial electronic landscape compared to the other sites.

Riga, Ventspils, and Liepaja exhibit similar mean EWF values and overlapping CPD distributions, indicating comparable average surface energetics. However, their differentiated and deconvoluted PEES spectra reveal progressively larger contributions near the valence-band onset compared to Salacgriva, indicating higher densities of localized electronic states. Among these sites, Liepaja displays the strongest and broadest spectral features, suggesting the highest degree of electronic heterogeneity, while Riga and Ventspils exhibit intermediate behavior.

The observed electronic trends are consistent with contrasting environmental regimes along the Latvian coast. Salacgriva is characterized by lower wave energy and stronger fluvial influence, conditions that may promote more stable surface terminations and reduced mechanical abrasion. In contrast, open Baltic Sea beaches experience higher hydrodynamic energy, which may enhance surface disorder, defect generation, and spatially heterogeneous charge distribution. While this interpretation is consistent with the electronic signatures observed, alternative factors such as subtle mineralogical impurities, grain-scale compositional variability, or microstructural differences cannot be excluded.

Overall, the results indicate that Baltic coastal sands share a common quartz-dominated electronic framework, while environmentally driven variations in near-edge electronic state density and surface potential organization produce meaningful differences in interfacial electronic behavior. Salacgriva sands represent the most electronically ordered case, whereas Riga, Ventspils, and particularly Liepaja exhibit increasingly defect-mediated and heterogeneous electronic characteristics. Future work is planned to focus on complementary morphological and chemical characterization to further correlate surface composition and microstructure with the electronic properties reported here.

5 Conclusion

This study presents a comparative evaluation of the surface electronic properties of quartz-rich coastal sands collected from four sectors of the Latvian Baltic Sea coast using PEES, EWF and KPFM measurements.

PEES analysis shows that all investigated sands exhibit characteristic spectral features with components centered at approximately 4.90, 5.28, and 5.48 eV. This may be associated with a shared quartz-dominated electronic structure, consistent with the intrinsic stability of SiO_2 . Site-specific differences are found to arise primarily from variations in peak areas and widths, which is connected to differences in the density and distribution of near-edge defect and surface-localised electronic states rather than changes in the bulk band structure.

EWF measurements reveal a narrow but systematic variation among the sampling sites. Salacgriva exhibits the lowest mean EWF with the smallest dispersion, while Riga, Ventspils, and Liepaja show higher and mutually overlapping

values. Statistical testing confirms that the Salacgriva EWF differs significantly from Riga and Liepaja. These results indicate that environmental conditions can measurably influence the energetic barrier for electron transfer at natural quartz sand surfaces.

KPFM measurements further highlight differences in nanoscale surface potential organization. Salacgriva sands display the highest and most uniform CPD values, along with a bimodal potential distribution, suggesting the presence of stable surface electronic configurations. In contrast, sands from Riga, Ventspils, and Liepaja show broader, Gaussian-like CPD distributions. This may indicate greater surface heterogeneity and more spatially variable charge organization for these locations.

Taken together, the results demonstrate that natural Baltic sands possess the essential electronic characteristics relevant for electron–ion exchange processes, while environmentally driven differences in near-edge electronic state density and surface potential organization influence the degree of order and heterogeneity of the surface electronic landscape. These findings contribute to a more detailed understanding of sediment–water interfacial behavior in coastal systems and provide a basis for future evaluation of natural sands in filtration, remediation, and related applications involving electrostatic and electron-mediated interactions.

References:

[1] Pope, G. A., Newly Discovered Submicron-Scale Weathering in Quartz: Geographical Implications, The Professional Geographer, Vol. 47, No. 4, 1995, pp. 375–387. https://doi.org/10.1111/j.0033-0124.1995.00375.x.

[2] Bregnhøj, M., Wili, N., Nielsen, A. B., Jensen, S. J. K., Nørnberg, P., Nielsen, N. Chr., Skibsted, J., & Finster, K., Triboelectrically Mediated Surface Reduction of Quartz Sand by Tumbling in Hydrogen Gas, The Journal of Physical Chemistry C, Vol. 129, No. 24, 2025, pp. 10900–10910. https://doi.org/10.1021/acs.jpcc.5c02082.

[3] Astaneh, A. G., Hosseinpour, I., Payan, M., Chenari, R. J., & Saeedi, N., Effect of Gradation, Size, and Shape of Particles on Quartz Sand–Geotextile Interface Properties, International Journal of Geosynthetics and Ground Engineering, Vol. 11, No. 4, 2025, pp. 1–15. https://doi.org/10.1007/s40891-025-00646-7.

[4] Garvie, L., Rez, P., Alvarez, J. R., Buseck, P. R., Craven, A. J., & Brydson, R., Bonding in alpha-quartz (SiO_2): A view of the unoccupied states, American Mineralogist, Vol. 85, No. 5–6, 2000, pp. 732–738. https://doi.org/10.2138/am-2000-5-611.

[5] Luo, A., & Chen, J., Effect of hydration and hydroxylation on the adsorption of metal ions on quartz surfaces: DFT study, Applied Surface Science, Vol. 595, 2022, pp. 153553–153563. https://doi.org/10.1016/j.apsusc.2022.153553.

[6] DelloStritto, M. J., Kubicki, J. D., & Sofo, J. O., Effect of Ions on H-Bond Structure and Dynamics at the Quartz(101)–Water Interface, Langmuir, Vol. 32, No. 44, 2016, pp. 11353–11365. https://doi.org/10.1021/acs.langmuir.6b01719.

[7] Schmidt, V., Senz, S., & Gösele, U., Influence of the Si/SiO_2 interface on the charge carrier density of Si nanowires, Applied Physics A, Vol. 86, 2007, pp. 187–191. https://doi.org/10.1007/s00339-006-3746-2.

[8] Buchanan, D., Fischetti, M., & DiMaria, D. J., Coulombic and neutral trapping centers in silicon dioxide, Physical Review B, Vol. 43, 1991, pp. 1471–1486. https://doi.org/10.1103/PhysRevB.43.147.

[9] DiMaria, D. J., The Properties of Electron and Hole Traps in Thermal Silicon Dioxide Layers Grown on Silicon, in S. T. Pantelides (Ed.), The Physics of SiO_2 and Its Interfaces, Pergamon Press, 1978, pp. 160–178. https://doi.org/10.1016/B978-0-08-023049-8.50034-8.

[10] Ye, C., Zhang, D.-S., Chen, B., Tung, C.-H., & Wu, L.-Z., Interfacial Charge Transfer Regulates Photoredox Catalysis, ACS Central Science, Vol. 10, No. 3, 2024, pp. 529–542. https://doi.org/10.1021/acscentsci.3c01561.

[11] Yuan, K., Rampal, N., Irle, S., Criscenti, L. J., Lee, S. S., Adapa, S., & Stack, A. G., Variations in proton transfer pathways and energetics on pristine and defect-rich quartz surfaces in water: Insights into the bimodal acidities of quartz, Journal of Colloid and Interface Science, Vol. 666, 2024, pp. 232–243. https://doi.org/10.1016/j.jcis.2024.03.144.

[12] Szymczycha, B., Zaborska, A., Bełdowski, J., Kuliński, K., Beszczyńska-Möller, A., Kędra, M., & Pempkowiak, J., The Baltic Sea, in World Seas: An Environmental Evaluation, Vol. II, Elsevier, 2019, pp. 85–111.

https://doi.org/10.1016/b978-0-12-805068-2.00005-x.

[13] Simonnin, P. G., Kerisit, S. N., Nakouzi, E., Johnson, T. C., & Rosso, K. M., Structure and Dynamics of Aqueous Electrolytes at Quartz (001) and (101) Surfaces, The Journal of Physical Chemistry C, Vol. 128, No. 16, 2024, pp. 6927–6940. https://doi.org/10.1021/acs.jpcc.4c00693.

[14] Pan, F., Liu, Z., Li, G., Zhang, Y., Fan, Z., Gang, Y., & Wang, D., Hydration Behavior of Quartz Surfaces Revealed by Molecular Dynamics Simulations with a Novel Machine Learning Potential, The Journal of Physical Chemistry C, Vol. 129, No. 33, 2025, pp. 14829–14840. https://doi.org/10.1021/acs.jpcc.5c03759.

[15] Li, D. Y., Guo, L., Li, L., & Lu, H., Electron Work Function – A Probe for Interfacial Diagnosis, Scientific Reports, Vol. 7, 2017, pp. 1–9. https://doi.org/10.1038/s41598-017-08841-x.

[16] Trukhin, A. N., & Fitting, H.-J., Investigation of Optical and Radiation Properties of Oxygen-Deficient Silica Glasses, Journal of Non-Crystalline Solids, Vol. 248, 1999, pp. 49–64. https://doi.org/10.1016/S0022-3093(99)00089-7.

[17] Giordano, L., Sushko, P. V., Pacchioni, G., & Shluger, A. L., Optical and EPR Properties of Point Defects at a Crystalline Silica Surface: Ab-initio Embedded-Cluster Calculations, Physical Review B, Vol. 75, 2007, pp. 1–12. https://doi.org/10.1103/PhysRevB.75.024109.

[18] Donglin, C., Shangli, D., Hai, L., & Xudong, Z., First-Principles Calculations of Electronic Structure and Optical Properties for Radiation-Induced Oxygen-Related Defects in Silica Glass, Journal of Non-Crystalline Solids, Vol. 666, 2025, pp. 123665–123675. https://doi.org/10.1016/j.jnoncrysol.2025.123665.

[19] Kang, H. C., Correlation between Bond Distortion and Band-Tail Electronic Density of States in Amorphous Silicon: A Tight-Binding Recursion Study, Journal of Non-Crystalline Solids, Vol. 261, 2000, pp. 169–180. https://doi.org/10.1016/S0022-3093(99)00592-X.

[20] Harirchi, P., Yang, M., & Kilin, D. S., Adsorption Mechanism of Carbonate Ion on the (111) Surface of Tricalcium Silicate through DFT Simulations, Molecular Physics, Vol. 123, No. ?, 2025, pp. 1–10. https://doi.org/10.1080/00268976.2025.2498607.

[21] Du, J., & Cormack, A. N., Molecular Dynamics Simulation of the Structure and Hydroxylation of Silica Glass Surfaces, Journal of the American Ceramic Society, Vol. 88, No. 9, 2005, pp. 2532–2539. https://doi.org/10.1111/j.1551-2916.2005.00352.x.

[22] Alfaridzi, R., Nugroho, B. S., & Rosandi, Y., Protonation Process of Porous Silica Cluster Surface Using Molecular Dynamics Method, POSITRON, Vol. 13, No. 1, 2023, pp. 14–22. https://doi.org/10.26418/positron.v13i1.63670

Contribution of Individual Authors to the Creation of a Scientific Article (Ghostwriting Policy)

Y.D. conceived and supervised the study and provided overall research guidance.
R.K., H.S. and M.G. contributed to the experimental design, data analysis, and manuscript preparation.
A.M. performed the photoelectron emission spectroscopy measurements and contributed to data analysis.
M.D. carried out the Kelvin probe force microscopy experiments and data analysis.
E.S. contributed to the analysis of PEES data, including spectral deconvolution.
S.R. contributed to data analysis and calculations.
I.K. conducted sample acquisition and preparation.
All authors have read and agreed to the published version of the manuscript.

Sources of Funding for Research Presented in a Scientific Article or Scientific Article Itself

This research was funded by the European Union Recovery and Resilience Facility project No. 5.2.1.1.i.0/2/24/I/CFLA/003.
Manuscript is part of the project C4835.ZPD.PI.0090.P1 “Purification of ship ballast water from heavy metal ions to reduce pollution”.

Conflict of Interest

The authors have no conflicts of interest to declare that are relevant to the content of this article.